International Journal of Mining Science and Technology 32 (2022) 551–561

Contents lists available at ScienceDirect

International Journal of Mining Science and Technology

journal homepage: www.elsevier.com/locate/ijmst

Trace element geochemistry and stable isotopic ($\delta^{13}C$ and $\delta^{15}N$) records of the Paleocene coals, Salt Range, Punjab, Pakistan

Noshin Masood [a], Tehseen Zafar [b,c], Karen A. Hudson-Edwards [d], Hafiz U. Rehman [e], Abida Farooqi [a,*]

[a] Environmental Geochemistry Laboratory, Department of Environmental Sciences, Faculty of Biological Sciences, Quaid-i-Azam University, PO 45320, Pakistan
[b] Institute of Geochemistry, Chinese Academy of Sciences, Guiyang 550081, China
[c] Institute of Geology, University of the Punjab, Lahore 54590, Pakistan
[d] Environment & Sustainability Institute and Camborne School of Mines, University of Exeter, TR10 9EZ, UK
[e] Graduate School of Sciences and Engineering, Kagoshima University, Kagoshima 890-0065, Japan

ARTICLE INFO

Article history:
Received 19 July 2020
Received in revised form 23 December 2021
Accepted 22 March 2022
Available online 30 March 2022

Keywords:
Coal
Salt Range
Pakistan
Geochemistry
Trace elements
$\delta^{13}C$ and $\delta^{15}N$ isotopes

ABSTRACT

The Paleocene coals of the Salt Range in the Punjab Province of Pakistan have great economic potential; however, their trace element and stable isotopic characteristics have not been studied in detail except for a few sporadic samples. In this study, a total of 59 coal samples of which 14 are obtained from open cast mines have been investigated for elemental composition and $\delta^{13}C$-$\delta^{15}N$ isotopic signatures. Average contents of trace elements such as Co, Cr, Cu, Pb, Sr, Th, U, V, and Zn are 7.4, 41.7, 11.2, 12.5, 90.2, 4.0, 1.9, 128, and 31.1 mg/kg, respectively. These values, when compared with the World Coal Clarke values, were relatively higher in low-rank coals in comparison with Clarke values for brown coals. Likewise, As (20.4 mg/kg), Co (6.6 mg/kg), Cr (22.4 mg/kg), Cu (13.3 mg/kg), Pb (19.2 mg/kg), Sr (154.7 mg/kg), Th (2.5 mg/kg), V (47.8 mg/kg), and Zn (75.1 mg/kg) were significantly higher in the sub-bituminous to bituminous coals of the Salt Range. Mineralogical analysis, based on X-ray diffraction and energy dispersive X-ray spectroscopy, revealed that the studied samples contain illite, kaolinite calcite, gypsum, pyrite, and quartz. Elemental affinity with organic and inorganic phases of coals calculated by an indirect statistical approach indicated a positive association of ash content with Ag, Al, Co, Cr, Cs, Cu, Mn, P, Rb, Pb, Th, U, and V, suggesting the presence of inorganic components in studied coals. However, As, Fe, Sr, and Zn exhibit negative correlations that imply their association with the organic fraction. The $\delta^{13}C$ and $\delta^{15}N$ isotopic range and average −24.94‰ to −25.86‰ (−25.41‰) and −2.77‰ to 3.22‰ (0.96‰), respectively, reflecting 3C type modern terrestrial vegetation were common in the palaeomires of studied coal seams. In addition, the trivial variations of 0.92‰ and 0.45‰ among ^{13}C and ^{15}N values can be attributed to water level fluctuations and plant assemblies.

1. Introduction

Coal deposits are a promising source of energy as well as an alternative source for many valuable chemical products [1–4]. Their utilization in the development and energy sector is linked with their intrinsic properties [5]. Coal characterization for its economical valorization is based on its chemical and petrographic analysis. As, Cd, Cr, Cu, Fe, Mn, Pb, Hg, Th, V, U, Se, Sn, Zn, and F^- are environmentally sensitive that could cause serious environmental pollution [6–10]. The elemental composition of coal is mainly characterized by different trace and major elements [5,11], among them As, Cd, Mo, Pb, Hg, B, Se, and Sn are priority pollutants and are found in higher concentrations in coal than the average value for the Earth's crust [12–15]. Based on the degree of volatilization, the potentially toxic trace elements within coals are classified into two groups (G1 and G2), e.g., [16]. Easily volatilized trace elements including As, Cd, Pb, Cu, and Zn are categorized as G1 while less volatilized elements such as Co, Cr, Mn, and V are consigned to G2 [16]. Other trace elements, such as Ni, are less abundant in coal; however, their significant enrichment in coal could cause emission problems during combustion as feeding coal or self-ignition in open cast mines [12–15,17]. As upon combustion, the volatile nature of these elements most likely concentrate their enrichment in the atmosphere and could cause severe As and Pb poisoning, for instance, black lung disease [18,19]. Major and trace elements in coal are mainly associated with carbonate, silicate, and sulfide minerals which can be liberated during

* Corresponding author.
E-mail address: afarooqi@qau.edu.pk (A. Farooqi).

https://doi.org/10.1016/j.ijmst.2022.03.007
2095-2686/

coal combustion and/or surface weathering via surface water (e.g., acid mine drainage); thus, these toxic elements could cause serious human health concerns [20–23]. The enrichment patterns of toxic elements principally occur during peat accumulation and coalification processes [24], which provide unique signatures to be used as geochemical indicators for their source interpretation, chemical cycling, and depositional environmental characteristics [25,26].

Stable isotopic ($\delta^{13}C$ and $\delta^{15}N$) signatures can be used to infer the composition of vegetation as well as changes that occur during early diageneses and coalification. For instance, $\delta^{13}C$ isotopic analysis of coals has been widely used to reconstruct the depositional environment such as environmental provenance, paleoclimate conditions, and atmospheric variations, and to determine the coal maceral's composition and origin [27,28]. In addition, isotope data can also address water level fluctuations during peat accumulation [28]. Moreover, $\delta^{13}C$ isotopic analysis reflects the common peat-forming vegetation within the palaeomires. Generally, $\delta^{13}C$ values for most coals mainly range between $-20‰$ to $-29‰$, relative to VPDB (Vienna Pee Dee Belemnite) standard values, which is in line with the range for modern 3C vegetation values of $-23‰$ to $-34‰$ [29]. The depositional environment greatly affects ^{13}C variations among the different plant tissues. For instance, the study of Grocke [30] revealed that lignin is less enriched in ^{13}C than cellulose [27,28]. Similarly, inertinite-rich coals show more negative ^{13}C values than vitrinite-rich coals [31]. Environmental changes occurring during peat accumulation such as air temperature, humidity, soil moisture, and precipitation rate can be detected using ^{13}C signatures. By contrast, the ^{15}N isotope signatures are mainly used to infer the organic matter sources and the peat-forming vegetation [28,32,33].

Pakistan is the seventh-largest coal-producing country globally and its indigenous coals are characterized by high volatile matter concentrations, high ash yield, and high sulfur content [34]. The three economically important coalfields in Pakistan are located in (1) the Salt Range and Makarwal in the Upper Indus Basin, (2) the Quetta-Kalat region in the Lower Middle Indus Basin, and (3) Hyderabad in Southern Sindh in the Lower Indus Basin (Fig. 1a). Coals in the Salt Range have been reported from three stratigraphic horizons. One occurs in the Permian Tobra Formation and the other two exist in the Paleocene Hangu and Patala Formations [35]. Permian coal in the Tobra Formation is confined to the western Salt Range whereas Late Paleocene coal in the Patala Formation occurs in the eastern and central Salt Range. Early Paleocene coal in the Hangu Formation is located at Makarwal in the Trans-Indus Salt Range (Fig. 2, [44]) [36,37]. Palynological studies of the Paleocene coals in the eastern, central, and Trans-Indus Salt Range have reported dinoflagellate cysts and pollen of the brackish-water palm genus Spinizonocolpites [38,39]. The coal petrography data show that the Salt Range coal samples were vitrinite-rich [38]. Likewise, the Trans-Indus coal seams are also vitrinite-rich [38]. The measured vitrinite reflectance value of these coals was ranged 0.62–1.0, which also reflects highly volatile bituminous B and C coal rank [40]. In addition, these coal beds have been developed under tropical to subtropical paleoclimatic conditions, that possess both dry and wet cycles [37]. The coal strata lie in Paleocene rocks in the central and eastern Salt Range and Trans-Indus Salt Range (Fig. 1b). According to the Geological Survey of Pakistan and the United States Geological Survey, joint reports (1984–1988), coal deposits of the main Salt and Trans-Indus Salt ranges were estimated to be 235 million metric tons [35,41]. In 2019, 800 small semi-mechanized coal mines were functional with an annual rate of extraction of 0.45 million metric tons.

Energy crises in Pakistan have forced the public/private sector to increase the utilization of both low and high-rank indigenous coals [34]. Only limited geochemical data for coals of the Salt Range, Pakistan are available so far [8,42,43]; however, when coal is evaluated for combustion, detailed quality analysis is required to characterize possible potential environmental issues that may arise during mining and the utilization of these coals. In addition, geological, chemical, and mineralogical characterization of Salt Range coals can provide more input on the mechanisms of formation and sources of trace element contents of the coal as well as their significance in terms of coal utilization. Therefore, the present study aims to geochemically characterize the Paleocene coals of the central and eastern Salt Range and Trans-Indus Salt Range to understand their trace elemental enrichment patterns, and their possible sources. The organic matter sources and depositional

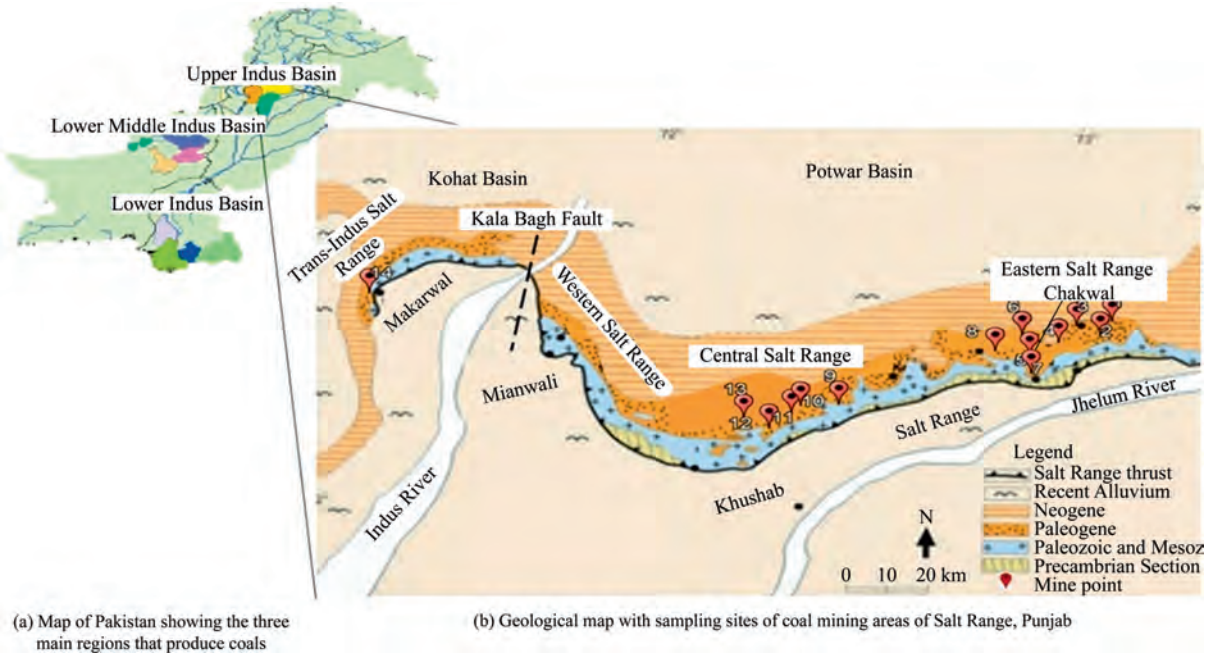

Fig. 1. Sampling locations of coal mining sites in Salt Range Punjab Pakistan.

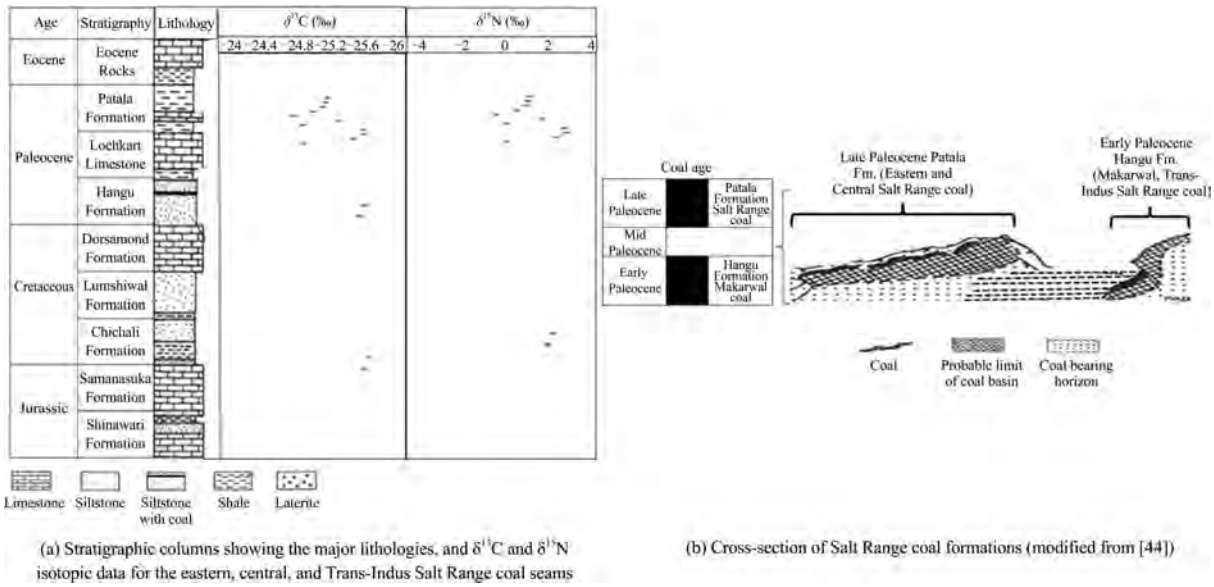

(a) Stratigraphic columns showing the major lithologies, and $\delta^{13}C$ and $\delta^{15}N$ isotopic data for the eastern, central, and Trans-Indus Salt Range coal seams

(b) Cross-section of Salt Range coal formations (modified from [44])

Fig. 2. Stratigraphic columns of Salt Range coal seams.

environments of the lignite and sub-bituminous to bituminous coals are also characterized using $\delta^{13}C$ and $\delta^{15}N$ isotopic data.

2. Geological setting

The Salt Range of Punjab is widely exposed at the foothills of the Himalayas and covers an area of about 250 km^2 [45]. It extends from the east of the Jhelum River to the west of the Indus River (Fig. 1b). Just beyond the Indus River, the N-S trending Kala Bagh Fault occurs (Fig. 1b). Here, the Indus River differentiates the Himalayan mountainous belt into two sections known as the Salt Range (lying between the Jhelum and Indus Rivers) in the east and the Trans-Indus Salt Range in the west (Fig. 1b). The Salt Range acted as a regional decollement for Paleozoic successions thrust over Neogene sediments of the Jhelum Plain in Pleistocene times. Within the Salt Range, a thick sedimentary cover, consisting of Precambrian to recent deposits, unconformably overlies low-grade metamorphic and igneous rocks [46].

The Paleocene coal seams in the main Salt Range occur in the Patala Formation that lies above the Ranikot Formation of Upper Paleocene age, whereas the coal seams at Makarwal occur in the Hangu Formation that underlies the Lockhart Limestone of Lower Paleocene age (Fig. 2). Singh et al. [47] reported a warm period followed by Paleocene-Eocene Thermal Maximum (PETM) that possibly caused diverse changes in the flora and fauna. Euxinic conditions, developed during the convergence of tectonic plates including Indian and Asian plates, blocked the Neotethys (an ocean that existed at the time) flow and increased the organic matter production that led to the peat accumulation [47].

The Patala Formation comprises claystone, siltstone, sandstone, mudstone, marl, limestone, carbonaceous shale, and coal beds [37]. In the eastern Salt Range, coal occurs in the form of thick lenses which are intercalated with shales and sandstones [35]. Currently, a single seam, known as the "Dandot coal seam" is being mined from different areas including Basharat, Dalwal, Khajula, Wahali, Wahula, Pidh, and Dandot (Fig. 1b). Similarly, coal seams of the central Salt Range are mined from Munarah, Padhrar, Katta Karli, and Arara (Fig. 1b).

The Makarwal coalfield (marked 14 on Fig. 1b) in the Mianwali District is in the Trans-Indus Salt Range extends from west of Kala Bagh to west of Makarwal (Fig. 1b). The estimated coal resources in the Trans-Indus Salt Range are 6.27 Mt, out of a total of 18.87 Mt in Makarwal. These coal resources form part of the Paleocene Hangu Formation. The Hangu Formation is composed of sandstones, and a lesser amount of mudstone, carbonaceous materials, claystone, coal beds, and limestone [38]. The coal beds are generally bright, resinous, pyritic, cleated, and gypsum infills cleats. The thickness of the coal seam varies from 0.5 to 3.5 m [35]. Makarwal coal seams show a transitional lithological depositional setting where laterite paleosols formed due to rising groundwater levels that converted the depositional basin into peatlands [38].

3. Sampling and methodology

Coal samples were collected for this study from three active (open cast) coal mine areas in the eastern Salt Range (District Chakwal), central Salt Range (District Khushab), and Trans-Indus Salt Range (District Mianwali). In total 59 samples (26 from eight coal mines from the Chakwal District (Basharat, Dalwal, Khajula, Wahali, Wahula, Pidh, and Dandot), 27 samples from five mines of Khushab area (including Munarah, Padhrar, Katta Karli, and Arara), and 6 samples from one mine of Makarwal (Mianwali) were selected for this study (Fig. 1b). Samples were collected by following the American Society for Testing and Materials (ASTM) (ASTM D6883-04 (2012) method, using a stainless-steel trowel and immediately storing the material in polythene bags to avoid oxidation and contamination. Before analysis, all samples were air-dried, milled to < 45 μm.

3.1. Geochemical analysis

For coal characterization, general parameters including moisture, volatile matter (VM), ash (the inorganic/mineral components of the coal samples), and fixed carbon content (C) on a dry basis were performed following the protocols of ASTM and the International Organization for Standardization (ISO) [48,49]. Total moisture content was determined using the ASTM D3173-11 method, and ash yield and volatile matter were determined using the ISO 1171:2010, ISO 562:2010 methods, respectively. Fixed carbon content (C in %) was calculated by difference [48] and results were measured as % by weight. Total sulfur (S) was determined using the Eschka method (ASTM, 2004, E 775–87) [50]. Whereas Hard-

grove grindability index was measured following the standard test method (ASTM D-409).

Four major (Al, Fe, Mn, P) and 14 trace elements (Ag, As, Cd, Co, Cr, Cs, Cu, Pb, Rb, Sr, Th, U, V, and Zn) were analyzed, using inductively coupled plasma mass spectrometry (ICP-MS) at Camborne School of Mines, University of Exeter, UK. Before analysis, samples were wet digested using concentrated HNO_3. For this process, 1 g of ground coal sample was digested with 5 mL concentrated HNO_3 for one hour in a heating block at 100 ℃. Samples were then allowed to cool and volumes were raised to 50 mL with ultra-pure Mili Q. After filtration with syringe filters (0.45 μm), samples were diluted 100 times using a 5% HNO_3 solution. The certified reference material STSD-2 used for quality control assurance gives precision and reproducibility of the instrument within the confidence limit of 98%.

Based on the World Coal Clarke values, enrichment patterns of major and trace elements of the studied coals were calculated using the concentration coefficient by Eq. (1) after [51,52].

$$CC = \frac{\text{Arithmetical means of elements in coal samples}}{\text{World Clarke value of coal's trace elements}} \quad (1)$$

CC < 1 indicates no enrichment. The enrichment CC > 1 in coal samples is further classified into significant enrichment (CC > 10), moderate enrichment (5 < CC < 10), and slight enrichment (2 < CC < 5). While metals with CC range of 0.5–2 were within the range of world average hard coal values [53].

Mineralogical compositions of selected bulk coal samples were determined by X-ray diffraction (XRD) using a Phillips PW 1710. The ground samples were analyzed using CuKα radiations (35 kV, 40 mA). Diffractograms were then obtained at the 2-theta range of 2.6°–70°, and peaks of the investigated samples were identified using the Bruker EVA1 software [54]. Chemical compositions were determined using an Energy Dispersive X-ray (EDX) Analyzer on a Scanning Electron Microscope (SEM). Before the EDX analysis, coal samples were crushed and made into pellets. These pallets were then coated with gold and examined under the SEM-EDX (JSM5910, JEOL) at Peshawar University. The accelerating voltage for the EDX was 10 kV, and the beam current was 40–60 mA during the operation.

3.2. Stable isotope analysis

For isotopic analysis, representative samples were crushed to < 45 μm. One gram of this material was measured into a precleaned tin capsule. The stable carbon and nitrogen isotopic signatures of these coal samples were analyzed in an isotope ratio mass spectrometer coupled with an elemental analyzer (SerCon 'Callisto CF-IRMS' system) at the Environment and Sustainability Institute, University of Exeter, UK. Results were expressed as delta notation (δ) in per mil scale (‰) using a standard equation (Eq. (2)).

$$\delta X = \left[\frac{R_{\text{sample}}}{R_{\text{standard}}} - 1\right] \times 1000 \quad (2)$$

where X is ^{13}C or ^{15}N; R_{sample} for C the $^{13}C/^{12}C$ ratio; and R_{standard} for C the $^{13}C/^{12}C$ value of the VPDB standard. For N, R_{sample} is the $^{14}N/^{15}N$ of samples and R_{standard} represents the $^{14}N/^{15}N$ value of air as the standard. For isotopic standards and drift correction, the National Institute of Standards and Technology (NIST) Standard Reference Material (SRM) 1577 Bovine Liver and two alanine standards were analyzed. The reproducibility of the results was 0.06‰ for C and 0.1‰ for N isotopic analysis (2 SD) [55].

3.3. Geo-statistical analysis

Trace elements were statistically analyzed to infer their enrichment patterns using MS Excel (Microsoft Office 365 ProPlus). The modes of occurrence of the trace elements in the coal samples were determined based on coefficient correlation using a multivariate statistical program (MVSP).

4. Results

4.1. Standard coal characteristics and rank

The results of the analysis of the general parameters of the coals are shown in Table 1. All the coals have low moisture content, i.e., 0.4%–1% (Table 1). Apart from the Katta Karli coal (No. 12 in Fig. 1b) in the central Salt Range, all other samples are classified as lower to medium ash coals. Higher ash contents (range 28%–51% by weight for central, 19.7%–39.8% by weight for the eastern part) in coals of Salt Range is mainly coincident with the complex coal seam composition that includes shale, sandstone, and siltstone partings present with the coal beds (Table 1) [56]. Coals of the Paleocene Patala Formation in the eastern and the central Salt Range have relatively higher contents of ash compared to the coals of the Hangu Formation in the Trans-Indus Salt Range, which most likely suggests an increase in the sediment influx during the peat accumulation period [37]. Compared with the Baluchistan and Sindh Province, coals of the Punjab Province have lower moisture and ash contents, and thus have more economic value (Fig. 3). Volatile matter and carbon content range from 16.7% to 39.6% by weight and 20% to 63% by weight for the eastern Range, 23.6% to 38.7% by weight and 9.2% to 44.8% by weight for the central Range, and 19% to 57% by weight and 10.1% to 61.1% by weight for coals of the Trans-Indus Salt Range, respectively. The sulfur values of eastern and Trans-Indus coals were lower than the central Salt Range coals. If we compare between the lignite and sub-bituminous type coals, then bituminous coals have higher S as opposed to that of lignite coals. The HGI values of lignite samples ranged between 35 and 50 that is following the HGI of lignite figured by Alpan [57,58]. However, sub-bituminous samples with more grindability showed higher HGI values [49]. The results of HGI analysis indicated that central Salt Range coals are hard whereas eastern and Trans-Indus Salt Range coals are relatively softer (Table 1).

Based on the proximate analysis, and gross calorific values (obtained from the ASTM D 38890; [36,49,58]), we could designate rank as lignite for the samples collected at Basharat (marked point 1, 2 in Fig. 1b), Dalwal (3), Wahali (5), and Wahula (6) mines, and bituminous from those at Pidh (7). Coal from the mines in the Dandot (marked 8 in Fig. 1b) and Khajula (4) areas in the eastern Salt Range were classified as sub-bituminous. Apart from Katta Karli (point 12 on Fig. 1b) (i.e., lignite type coal), the remaining coal samples in the central Salt Range were also classified as sub-bituminous. Based on these results, coals of the Patala Formation in the eastern and central Salt Range are ranked as lignite and high volatile bituminous. Similarly, coal from the Trans-Indus Salt Range, due to its high volatile content, is categorized as sub-bituminous. Hence, based on the ASTM (D 38890 ranking), the low-grade indigenous coal of the Salt Range, Punjab, with low moisture and high carbon and ash content could be blended with high-quality imported coals to improve their energy efficiency (Table 1), as suggested earlier by Rehman et al. [36].

4.2. Occurrence and enrichment of major, trace elements and their interpretations

A comparison of concentrations of trace elements measured in lignite (N = 21) and sub-bituminous to bituminous coals (N = 38) against the World Coal Clarke values [52] is given in Table 2. Among the 14 analyzed trace elements in the coal of the Paleocene Patala Formation, average concentrations of As, Co, Cr, Pb, Sr, Th, U,

Table 1
Concentrations of general/proximate parameters, Hardgrove grindability index (HGI), and coal classification.

Location	Mine site	*N*	Moisture (%)	VM (%)	Ash (%)	C (%)	Total S value (kcal/kg)	HGI	Rank
Eastern Salt Range	Pidh	2	0.7	16.7	19.7	63.0	3.80	73	Bituminous
	Basharat	6	0.9	39.6	39.6	20.0	5.70	48	Lignite
	Dandot	3	0.6	30.3	34.8	34.4	3.90	76	Sub-bituminous
	Khajula	4	0.4	32.0	30.3	37.3	3.70	74	Sub-bituminous
	Dalwal	6	0.8	38.6	39.8	20.8	5.90	44	Lignite
	Wahali	3	0.8	38.6	39.8	20.8	5.60	47	Lignite
	Wahula	2	1.0	36.0	36.5	26.5	5.30	49	Lignite
Central Salt Range	Padhrar	12	0.9	23.6	34.8	40.7	8.24	57	Sub-bituminous
	Munarah	6	0.9	26.2	34.3	38.6	6.80	63	Sub-bituminous
	Katta Karli	3	0.8	38.7	51.3	9.2	5.10	49	Lignite
	Arara	6	0.9	26.5	28.0	44.8	6.90	61	Sub-bituminous
Trans-indus Salt Range	Makarwal	6	1.0	28.8	28.0	48.1	4.50	92	Sub-bituminous

Note: *N* is the sample number.

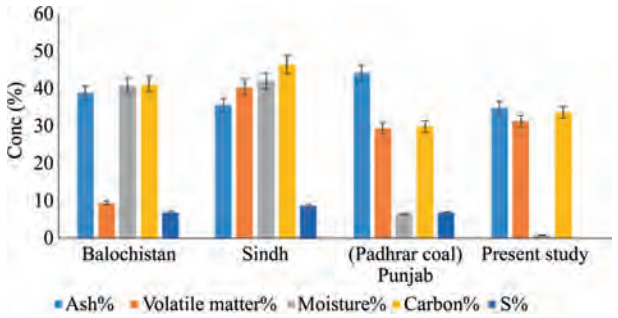

Fig. 3. Comparison of proximate analysis of present study area with other local coal [59]. *Error bars depict the precision of the calculations.

V, and Zn were significantly higher in lignite of the eastern Salt Range compared to those in the other areas (Table 2). Lignite samples in the Patala Formation of the central Salt Range have relatively high concentrations of Mn (64.2 mg/kg). Sub-bituminous to bituminous samples of the same Formation in the central Salt Range are enriched in Co, Cr, Pb, Sr, Th, V, and Zn, whereas the high-volatile bituminous C-type samples of the Hangu Formation in the Trans-Indus Salt Range (at Makarwal) display elevated concentrations of As, Cd, Cr, Cu, Pb, Th, V, and Zn. These elevated concentrations suggest an association of the elements with the inorganic affinity (as will be discussed in Sections 5.1 and 5.2). Arsenic, Cd, Cu, Pb, and Zn were likely associated with sulfides [54], Cr and Co with siderophile elements, and Th, U, and V with other lithophile elements in the coal [60]. Average contents of Cs, P, and Rb in both lignite and sub-bituminous to bituminous samples were much lower than the World Coal Clarke values (Table 2).

The calculated concentration coefficient for the major and trace elements shows that Al, Cs, P, Rb, and U (except Dalwal) in all the selected samples were < 1 indicating no enrichment for these ele-

Table 2
Average major and trace element concentrations (in mg/kg) and the World Clarke values of the studied samples.

	Mine site	*N**	Ag	Al	As	Cd	Co	Cr	Cs	Cu	Fe
ESR	Pidh	2	0.1	847	5.4	0.1	5.4	34.1	0.1	10.1	26260
	Basharat 1	2	0.0	729	3.4	0.1	4.1	21.9	0.2	15.7	25113
	Basharat 2	4	0.0	707	2.0	0.1	2.8	20.2	0.4	14.0	14933
	Wahali	3	0.0	957	4.2	0.1	8.3	27.8	0.1	9.9	49725
	Wahula	2	0.0	631	19.0	0.1	15.7	26.5	0.1	9.7	48695
	Khajula	4	0.1	1167	5.3	0.1	7.7	23.1	0.2	13.7	37969
	Dandot	3	0.0	550	4.3	0.2	4.6	24.5	0.1	15.3	35636
	Dalwal	6	0.0	870	6.4	0.1	8.5	74.8	0.1	9.1	21299
CSR	Padhrar 1	6	2.3	742	20.2	0.2	6.2	16.5	0.1	13.0	82391
	Padhrar 2	6	0.6	1808	33.9	0.3	9.9	29.2	0.1	12.8	111485
	Munarah	6	0.0	1697	49.9	0.7	12.0	23.0	0.1	9.5	79888
	Katta Karli	3	0.2	1742	4.2	0.1	2.9	30.5	0.1	10.0	17013
	Arara	6	0.0	1085	3.8	0.1	3.1	15.0	0.1	9.8	16059
TSR	Makarwal	6	0.1	1342	17.3	0.1	2.4	23.1	0.2	21.2	30566
World Coal Clarke value**			0.1	82300***	8.3	0.2	5.1	16.0	1.0	16.0	56000***
	Mine Site	*N**	Mn	P	Pb	Rb	Sr	Th	U	V	Zn
ESR	Pidh	2	23.8	0.0	15.2	0.4	199	5.7	1.3	85.1	27.8
	Basharat 1	2	37.8	0.0	7.6	1.1	79.0	3.7	1.8	42.9	30.5
	Basharat 2	4	21.5	0.0	5.4	1.7	96.2	3.5	1.0	25.4	22.9
	Wahali	3	48.6	0.0	13.3	0.7	57.1	3.5	1.9	39.8	30.7
	Wahula	2	72.6	0.0	18.7	0.5	73.8	3.4	1.3	69.6	34.4
	Khajula	4	58.2	0.0	14.2	1.5	187	3.7	1.7	40.4	28.5
	Dandot	3	42.3	0.0	16.6	0.7	90.9	3.1	1.2	49.6	90.1
	Dalwal	6	25.0	0.0	16.4	0.4	112	4.9	2.7	289	35.8
CSR	Padhrar 1	6	104	16.4	23.7	0.6	143	2.6	1.2	49.9	46.2
	Padhrar 2	6	77.4	10.4	32.4	0.6	171	1.6	1.3	70.9	65.0
	Munarah	6	106	2.7	31.3	0.6	287	1.8	1.1	60.3	171
	Katta Karli	3	64.2	0.0	15.7	1.6	145	2.9	1.1	46.8	40.4
	Arara	6	35.5	0.0	7.5	0.6	115	1.5	0.8	23.4	65.9
TSR	Makarwal	6	22.3	0.0	7.3	1.4	53.5	2.9	1.3	25.9	66.9
World Coal Clarke value			86.0	230	7.8	14.0	110.0	3.3	2.4	25.0	23.0

Notes: **N*: sample number; **World Clarke value source [52]; ***Values extracted from [64]; ESR - eastern Salt Range; CSR - central Salt Range; and TSR - Trans-Indus Salt Ran.

ments (Fig. 4). However, coals of the eastern Salt Range were enriched in Co (except Basharat and Dandot), Cr, V, Pb, Th, and Zn. In comparison, coals of Dalwal displayed significant V enrichment and those of Wahula showed slight enrichment in As and Co, all of which could be of environmental concern [61], as these elements are identified as hazardous air pollutants (HAP_S) by U.S. Environmental Protection Agency (US-EPA), 1990 [62]. Coals of the central Salt Range are enriched in Co, Cr, Fe, Mn, Sr, V, and Zn and considerably enriched in As, Cd, and Pb. In addition, the coals of Padhrar were significantly enriched in Ag (CC = 15), and those from Munarah were significantly enriched in As (CC = 6) and Zn (CC = 7.4). Trans-Indus Salt Range coals were moderately enriched in Cr, Cu, V, and Zn. Overall, the studied samples from the Salt Range show relatively high enrichment in Ag, As, Cr, Pb, V, and Zn (Fig. 4). These environmentally toxic elements pose potential risks and may cause serious environmental and health concerns (e.g., mutagenic, carcinogenic, and teratogenic effects) [20,63].

5. Discussions

5.1. Mineral assemblages

The identified minerals by XRD and SEM-EDX in coals of the central and eastern Salt Range are silicates (quartz, kaolinite, feldspar, and illite), carbonates (main calcite), and sulfides (pyrite) (Fig. 5). The XRD analysis confirmed quartz as the most abundant mineral phase in the samples from all parts of the Salt Range. This likely reflects the quartz-rich sandstone as a dominant sediment source in the Salt Range because it is interbedded with coals [35]. Kaolinite was the second most abundant mineral in the studied coal samples of the Patala Formation in eastern Salt and central Salt Ranges, whereas pyrite was the second most abundant mineral after quartz in the Hangu Formation of the Trans-Indus Salt Range (Fig. 5). Furthermore, carbonate minerals, and sulfides mainly pyrite, were likely the major sources of the inorganic content of the coals in the central and eastern Salt Range (Tables 1 and 2) [65,66]. It is widely reported that the gypsum most likely forms as a result of the reaction of sulfuric acid (product of pyrite oxidation) with Ca^{2+} [24], evaporation of porewater [14,67], or by precipitation of calcium and sulfate during peat deposition and epigenetic stage [68]. Therefore, the presence of gypsum in the TSR site of this study most likely developed owing to the reaction of sulfuric acid with Ca^{2+} [24] or mainly can be attributed to precipitation of calcium and sulfate during the phase of peat accumulation or early diagenetic stages (Fig. 5).

5.2. Controlling factors on elemental compositions

To understand the occurrence of minerals in host coals and to support the XRD results, EDX analysis was also performed. The EDX spectra of the studied coal samples show contrasting peaks of C, Al, S, Si, Fe, S, O, and traces of K and Mg (Fig. 6). Iron and S mainly show their association and sole source from pyrite, whereas sources of Si and Al in the studied coals can be attributed to aluminosilicate minerals such as kaolinite and illite. Silica also reflects

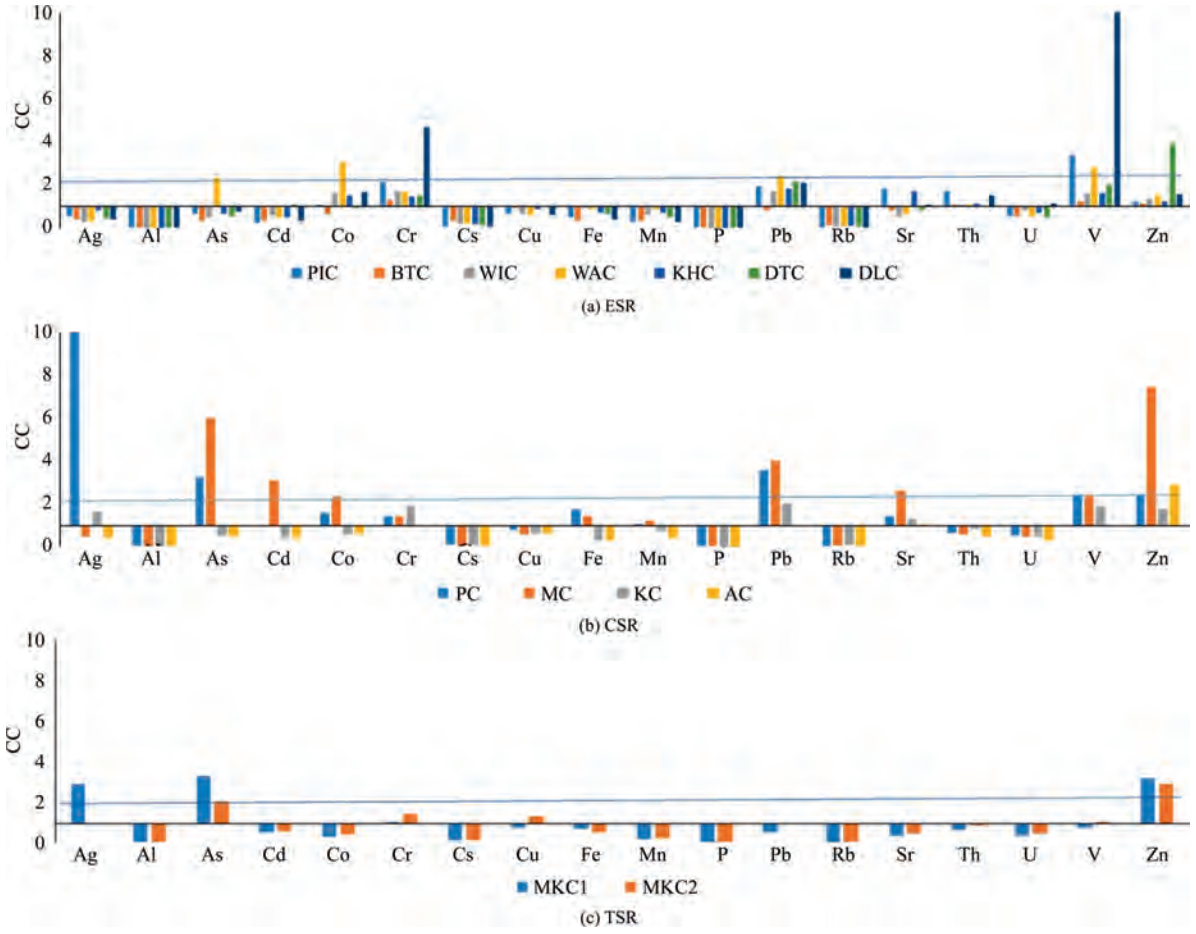

Fig. 4. Enrichment coefficients of environmentally sensitive trace elements of coals of Salt Range relative to the World Coal Clarke values [52]. PIC - Pidh coal, BTC - Basharat, WIC - Wahali, WAC - Wahula, KHC - Khajula, DTC - Dandot, DLC - Dalwal, PC - Padhrar, MC - Munarah, KC - Katta Karli, AC - Arara, and MKC - Makarwal coal.

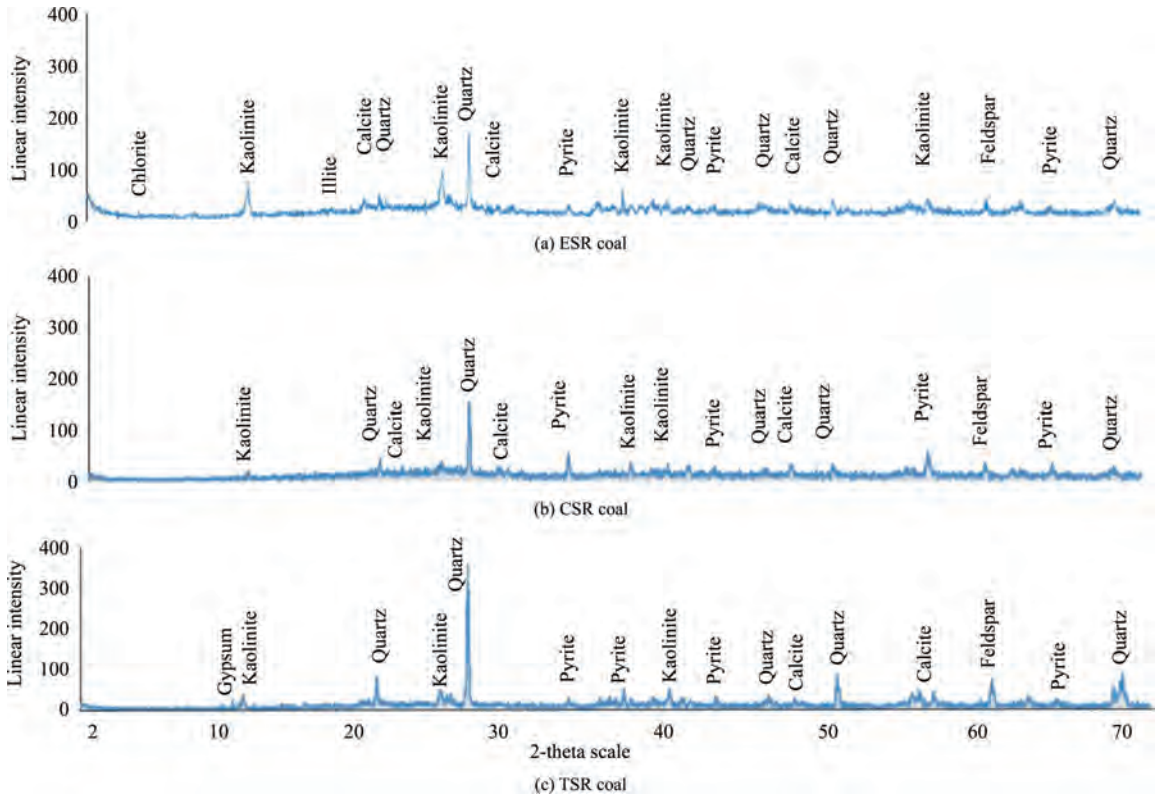

Fig. 5. XRD patterns of the studied coal samples. ESR indicates eastern Salt Range; CSR indicates central Salt Range; and TSR indicates Trans-Indus Salt Range.

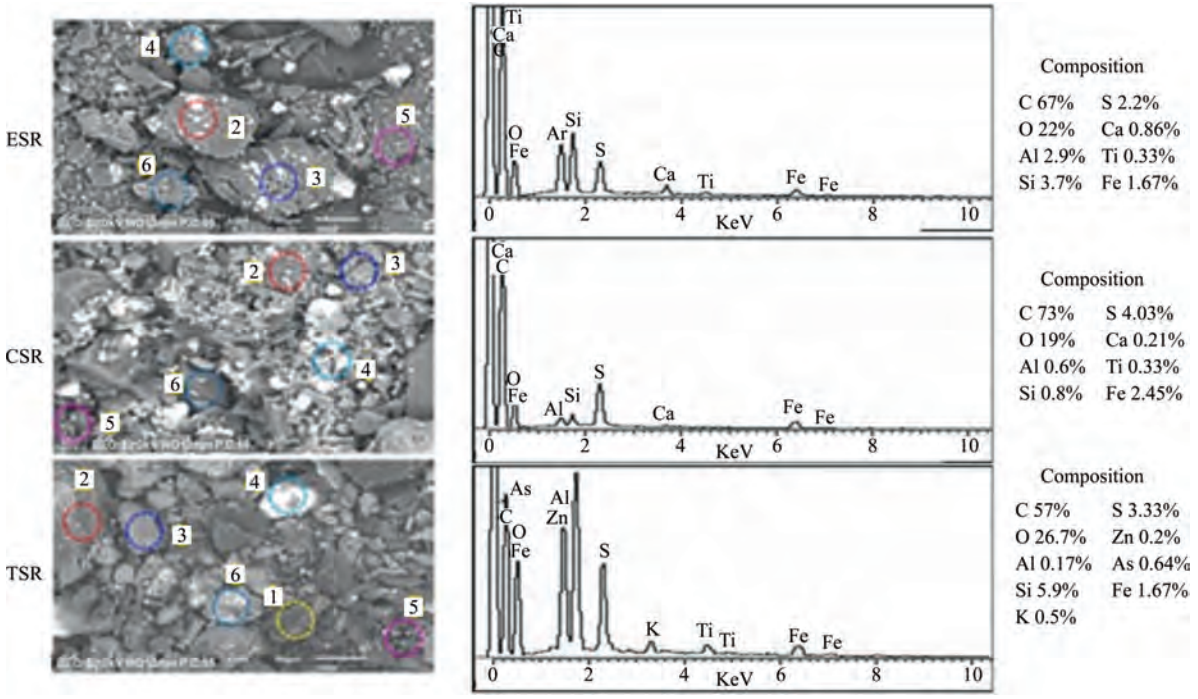

Fig. 6. Back-scattered electron with energy dispersive X-ray spectroscopy (BSE-EDX) patterns and elemental composition (%) of constituent minerals in samples of eastern Salt Range (ESR), central Salt Range (CSR), and Trans-Indus Salt Range (TSR) coal samples. Circles with numbers in representative samples indicate the analyzed spots for main minerals: 1 - gypsum; 2 - pyrite; 3 - calcite; 4 - quartz; 5 - alumino-silicate (clays); and 6 - feldspar.

the signatures of quartz. Calcium in the investigated coals is mainly derived from carbonates and sulfates specifically calcite and gypsum, respectively. These results are in good agreement with the XRD analysis (Fig. 5), where the most common minerals observed in the studied coal samples are quartz, illite, kaolinite, feldspar, gypsum, pyrite, and calcite that are mainly comprised of Al, Si, Fe, S and Ca (Fig. 6).

Statistical tools such as correlation coefficients can also reveal the geochemical affinities of the different trace elements with each other and with their respective mineralogy. The correlation coefficient between trace elements and ash contents also reflects their organic and inorganic affinities (Fig. 7). Positive correlations between trace elements including Ag, Al, Co, Cr, Cs, Cu, Mn, P, Rb, Pb, Th, U, and V and ash contents suggest that they were largely hosted in the inorganic fractions of the coal (Fig. 7) [11,69,70]. By contrast, As, Fe, Sr, and Zn exhibit weak negative relationships with ash contents, suggesting their affinity with the organic components of the coal (Fig. 7) [20,71]; however, Fe-bearing minerals were considered the main source of various elements. Positive correlations between Fe and Pb, As, and Mn revealed that these elements were most probably related with sulphides, particularly pyrite grains in the studied samples (Table 3) [72]. Arsenic significantly positively correlated with Fe, Pb, and Zn, and a weak positive correlation with other toxic metals such as Cd, Co, and Mn suggested that it may have been derived from the same source i.e., sulfide (Table 3) [73]. Similarly, a strong positive correlation of Cr with Th, U, and V, Th with U and V, Rb with Cs, and Mn with P, Al suggests that aluminosilicates were the major host of Rb, Cr, and Th, U, Cs, and V (Table 3) [14].

Table 3
Correlation coefficient (r) of trace elements and Ash content of coals of the studies coal samples.

r	Ash content
$0.7 < r < 1.0$	Mn vs P, As vs Pb, Cr vs V & U, Zn vs Cd, U vs V, Rb vs Cs
$0.5 < r < 0.7$	As vs Fe & Zn, Fe vs Pb, Sr vs Al, Co vs Pb & Co, Th vs Cr, U, &V
$0 < r < 0.5$	Ash vs Mn, P, & U, As vs Cd & Co

5.3. $\delta^{13}C$ and $\delta^{15}N$ isotopic compositions

Stable carbon and nitrogen isotope data (N=12) ranged from −24.94‰ to −25.86‰ for ^{13}C and −2.77‰ to 3.22‰ for ^{15}N respectively (Fig. 8). Plant sources, coalification, and peatification processes were the likely factors that influenced the stable isotope signatures [74,75]. Coal samples having higher $\delta^{13}C$ values indicate peat-forming vegetation mainly comprises cellulose and carbohydrates, whereas relatively lower $\delta^{13}C$ values suggest the involvement of lignin and lipids [30]. Organic matter (OM) derived from the terrestrial woody vegetation comprises a considerable amount of carbon-containing lignocellulose compounds; hence, these compounds are depleted in algal and planktonic sources [76]. The $\delta^{13}C$ range of −24.94‰ to −25.86‰ for the studied coal samples is comparable to that of the modern terrestrial land vegetation i.e. woody plants (−23‰ to −34‰) [27]. Likewise, the $\delta^{15}N$ values of −2.77‰ to 3.22‰ also lie within the range of modern terrestrial plants (i.e., 0‰–2‰) [76,77]. Thus, stable isotopic signatures of the lignite and sub-bituminous to bituminous coals samples indicate higher terrestrial plants were the possible source of the coal OM (Fig. 8). The $\delta^{13}C$ concentrations of the OM derived from C_3 vascular plants and C_3 aquatic plants range between −22‰ to −33‰, and −13‰ to −27‰ respectively [78]. Upon plotting ^{13}C values of the studied coal against C_3 terrestrial plants and C_3 aquatic plants, the studied samples fall under the terrestrial plant range (Fig. 8).

Data obtained from the studied samples showed a negligible shift in ^{13}C enrichment (Fig. 8) falling within the range of the Calvin/C_3 cycle of photosynthesis (−33‰ to −22‰). Similarly, OM contents obtained from the terrestrial vegetation exhibited lower nitrogen enrichment (0‰–2‰), whereas planktonic sources usually yield a value of + 8‰ [76]. Hence, the $\delta^{13}C$ and the $\delta^{15}N$ signatures of the studied samples did not show significant variation with increasing rank (Fig. 8).

The reported stable isotopic values are also very with gymnosperm plants (average $\delta^{13}C$ value is −25.41‰) [28,79,80]. The slight fluctuations in the ^{13}C isotopic values of the studied coals (i.e., −24.94‰ to −25.86‰) probably reflect transient climatic conditions during the formation of the OM (Fig. 8) [29]. Tropical to subtropical and warm climates characterize the Paleocene [37,38], and show that peat-forming C_3 type vegetation grew under a shallow marine (e.g., mangrove) and deltaic depositional environment. The peatland formation along the margins of the Tethys Sea experienced regressive and subsequent transgressive phases during the Paleocene time when water level fluctuations possibly caused wet and drier cycles. These changes in the environmental conditions are indicated by variation in carbon isotopes (Fig. 8). Such marine sediments are characterized by the high concentrations of As, U, and other trace elements [81]. Furthermore, the deltaic coals, particularly coals related with pleiomeric deposited under lower delta plain conditions, could display higher ash yields and concentrations of aluminosilicate affiliated elements due to high detrital input. Higher concentrations of As, Co, Cr, Cu, Pb, Sr, Th, U, V, and Zn traced in the present study coals also showed the same evidence (Table 2). Similarly, declines in the N enrichment can be associated with the increase in average precipitation [76]. Such higher rainfall and subsequent changes in water levels most likely caused the higher fractionation of the lighter N isotope (^{14}N) relative to the heavier ^{15}N (Fig. 8) [32,82]. Therefore, $\delta^{13}C$ and $\delta^{15}N$ signatures of the studied coal samples suggest that tropical to subtropical and warm climate and sea-level fluctuations may have developed the peat mire. This depositional environment could have also caused the abundance of either inertinite or vitrinite macerals that induced the ^{13}C variability in the studied coals [28,31].

Coal facies analysis (maceral compositions) can further indicate the environmental conditions of the peatification process [73]. For instance, the abundant vitrinite (79% and 71%), and the inertinite contents of 11% and 18% in the Patala and Hangu formations, respectively further signify the presence of woody tissues representing wet climatic conditions in the Salt Range coals during their formation [37,38,83,84]. In addition, the vitrinite enrichments suggested by the $\delta^{13}C$ signatures of the studied coals imply the wet

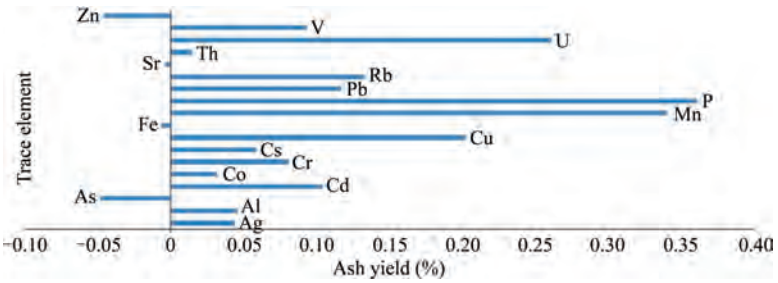

Fig. 7. Correlation coefficients of trace elements with ash yield for the studied samples.

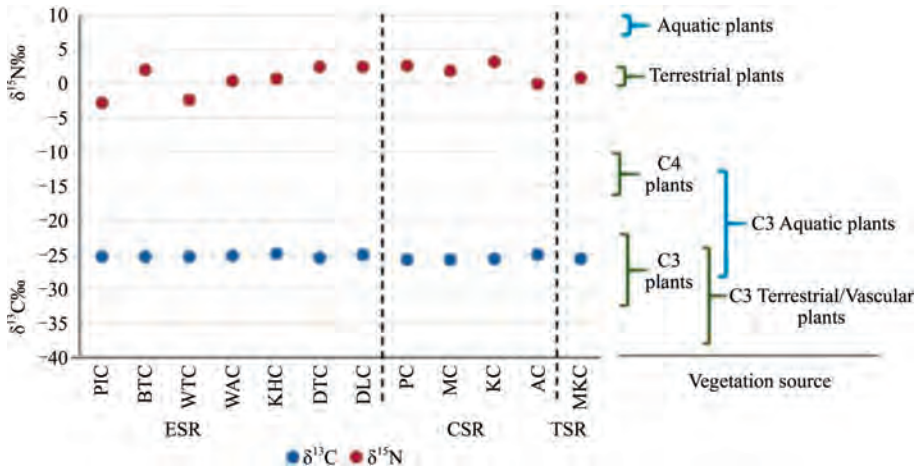

Fig. 8. Stable isotope signature and vegetation sources of organic matter.

and anoxic environment for peatification existed [78]. Based on these observations the stable isotopic composition of the investigated coal samples may have been regulated by water table level fluctuations which in turn influenced maceral composition and C3 plant type.

6. Conclusions

Based on information obtained from the elemental contents and stable isotope values from the studied coal samples the following conclusions can be made:

(1) The studied coal seams in the Salt Range and the Trans-Indus Salt range are lignite and sub-bituminous to bituminous types.
(2) Average concentrations of Co, Cr, Cu, Pb, Sr, Th, U, V, and Zn in lignite and As, Co, Cr, Cu, Pb, Sr, Th, V, and Zn in the sub-bituminous to bituminous coals of the Salt Range were significantly higher than the World Clarke values. Arsenic Cd, Cr, Cu, Pb, Th, V, and Zn of the Trans-Indus Salt Range coals are also higher than the World Clarke values. The elevated levels of environmentally sensitive trace elements could cause human health concerns that need to be addressed.
(3) Mineral assemblages are characterized by silicates (quartz, feldspar, and other clay minerals), carbonates (calcite), sulfates (gypsum), and sulfides (pyrite). The carbonate, sulfide, and sulfate mainly host the potentially toxic elements.
(4) The occurrence of major/trace elements in lignite and hard coals has been studied using indirect evidence. Positive correlation coefficients of trace elements with ash yields suggest inorganic affiliations for the trace elements. The continuous use of these coals in the industry most likely enriches the environment with relatively high concentrations of potentially toxic elements.
(5) Stable $\delta^{13}C$ ($-24.94‰$ to $-25.86‰$) and $\delta^{15}N$ ($-2.77‰$ to $3.22‰$) isotopic signatures suggest that C_3 type plants grew under restricted marine and deltaic depositional environments and were responsible for peat formation. The small variations among these isotopic values were likely due to water level fluctuations and plant communities as well as maceral compositions.
(6) Based on the geochemistry and enrichment pattern of trace elements in the tested coals, detailed studies regarding leaching experiments and elemental compositions of different grain sizes are highly recommended to understand coal beneficiation as well as possible negative environmental aspects.

Acknowledgements

This manuscript is part of the Ist author's Ph.D. dissertation. We would like to thank the Higher Education Commission Pakistan for funding the lab research under its International Research Support Initiative Program (IRSIP) program, the Department of Environmental Science, Quaid-i-Azam University, Islamabad (especially Environmental Hydro geochemistry Lab), and the Environment & Sustainability Institute and Camborne School of Mines, University of Exeter, for technical support in conducting lab analysis.

References

[1] Dai SF, Finkelman RB. Coal as a promising source of critical elements: Progress and future prospects. Int J Coal Geol 2018;186:155–64.
[2] Feng JJ, Wang EY, Huang QS, Ding HC, Zhang XY. Experimental and numerical study of failure behavior and mechanism of coal under dynamic compressive loads. Int J Min Sci Technol 2020;30(5):613–21.
[3] Emery J, Canbulat I, Zhang CG. Fundamentals of modern ground control management in Australian underground coal mines. Int J Min Sci Technol 2020;30(5):573–82.
[4] Zhou J, Chen C, Wang MZ, Khandelwal M. Proposing a novel comprehensive evaluation model for the coal burst liability in underground coal mines considering uncertainty factors. Int J Min Sci Technol 2021;31(5):799–812.
[5] Onifade M, Lawal AI, Abdulsalam J, Genc B, Bada S, Said KO, Gbadamosi AR. Development of multiple soft computing models for estimating organic and inorganic constituents in coal. Int J Min Sci Technol 2021;31(3):483–94.
[6] Shan Y, Wang WF, Qin Y, Gao LS. Multivariate analysis of trace elements leaching from coal and host rock. Groundw Sustain Dev 2019;8:402–12.
[7] Schweinfurth S. Chapter C: An introduction An introduction to coal quality (20 pp). USGS Professional Paper 1625-F: The National Coal Resource Assessment Overview. US Geological Survey 2009.
[8] Ali J, Kazi TG, Baig JA, Afridi HI, Arain MS, Ullah N, Arain SS, Siraj S. Monitoring of arsenic fate with proximate parameters and elemental composition of coal from Thar coalfield. Pakistan J Geochem Explor 2015;159:227–33.
[9] Singh PK, Rajak PK, Singh MP, Singh VK, Naik AS. Geochemistry of kasnau-matasukh lignites, nagaur basin, Rajasthan (India). Int J Coal Sci Technol 2016;3(2):104–22.
[10] Prachiti PK, Manikyamba C, Singh PK, Balaram V, Lakshminarayana G, Raju K, et al. Geochemical systematics and precious metal content of the sedimentary horizons of Lower Gondwanas from the Sattupalli coal field, Godavari Valley. India Int J Coal Geol 2011;88(2–3):83–100.
[11] Chehreh CS. Exploring relationships of gross calorific value and valuable elements with conventional coal properties for North Korean coals. Int J Min Sci Technol 2019;29(6):867–71.
[12] Equeenuddin SM, Tripathy S, Sahoo PK, Ranjan A. Geochemical characteristics and mode of occurrence of trace elements in coal at West Bokaro coalfield. Int J Coal Sci Technol 2016;3(4):399–406.

[13] Dai SF, Hower JC, Finkelman RB, Graham IT, French D, Ward CR, Eskenazy G, Wei G, Zhao L. Organic associations of non-mineral elements in coal: A review. Int J Coal Geol 2020;218:103347.
[14] Finkelman RB, Dai SF, French D. The importance of minerals in coal as the hosts of chemical elements: A review. Int J Coal Geol 2019;212:103251.
[15] Karayigit AI, Gayer RA, Querol X, Onacak T. Contents of major and trace elements in feed coals from Turkish coal-fired power plants. Int J Coal Geol 2000;44(2):169–84.
[16] Guo SQ. Trace elements in coal gangue: A review. In: Contributions to Mineralization. InTech; 2018.
[17] Song XY, Shao LY, Yang SS, Song RY, Sun LM, Cen SH. Trace elements pollution and toxicity of airborne PM_{10} in a coal industrial city. Atmos Pollut Res 2015;6 (3):469–75.
[18] Finkelman RB, Orem W, Castranova V, Tatu CA, Belkin HE, Zheng BS, Lerch HE, Maharaj SV, Bates BL. Health impacts of coal and coal use: possible solutions. Int J Coal Geol 2002;50(1–4):425–43.
[19] Zhou CC, Liu GJ, Cheng SW, Fang T, Lam PKS. The environmental geochemistry of trace elements and naturally radionuclides in a coal gangue brick-making plant. Sci Rep 2014;4:6221.
[20] Dai SF, Ren DY, Chou CL, Finkelman RB, Seredin VV, Zhou YP. Geochemistry of trace elements in Chinese coals: a review of abundances, genetic types, impacts on human health, and industrial utilization. Int J Coal Geol 2012;94:3–21.
[21] Masood N, Hudson-Edwards KA, Farooqi A. Groundwater nitrate and fluoride profiles, sources and health risk assessment in the coal mining areas of Salt Range, Punjab Pakistan. Environ Geochem Heal 2021:1–14.
[22] Masood N, Hudson-Edwards K, Farooqi A. True cost of coal: coal mining industry and its associated environmental impacts on water resource development. J Sustain Min 2020;19(3):135–49.
[23] Zhu M, Bazai NA, Li XL, Huang MN, Muhammad T, Lei M, Wang H. Research on wetland ecological restoration of coal mining subsidence area in Suzhou, China. Fresenius Environ Bull 2017;26(8):5177–83.
[24] Ward CR. Analysis and significance of mineral matter in coal seams. Int J Coal Geol 2002;50(1–4):135–68.
[25] Dai SF, Bechtel A, Eble CF, Flores RM, French D, Graham IT, et al. Recognition of peat depositional environments in coal: A review. Int J Coal Geol 2020;219:103383.
[26] Tu QY, Cheng YP, Xue S, Ren T, Cheng X. Energy-limiting factor for coal and gas outburst occurrence in intact coal seam. Int J Min Sci Technol 2021;31 (4):729–42.
[27] Rimmer SM, Rowe HD, Taulbee DN, Hower JC. Influence of maceral content on $\delta^{13}C$ and δ15N in a Middle Pennsylvanian coal. Chem Geol 2006;225(1–2):77–90.
[28] Liu JJ, Dai SF, Hower JC, Moore TA, Moroeng OM, Nechaev VP, Petrenko TI, French D, Graham IT, Song XL. Stable isotopes of organic carbon, palynology, and petrography of a thick low-rank Miocene coal within the Mile Basin, Yunnan Province, China: implications for palaeoclimate and sedimentary conditions. Org Geochem 2020;149:104103.
[29] Ding DS, Liu GJ, Fu B. Influence of carbon type on carbon isotopic composition of coal from the perspective of solid-state ^{13}C NMR. Fuel 2019;245:174–80.
[30] Grocke DR. The carbon isotope composition of ancient CO_2 based on higher-plant organic matter. Philos Trans Royal Soc Lond Ser A Math Phys Eng Sci 2002;360(1793):633–58.
[31] Moroeng OM, Wagner NJ, Hall G, Roberts RJ. Using $\delta^{15}N$ and $\delta^{13}C$ and nitrogen functionalities to support a fire origin for certain inertinite macerals in a No. 4 Seam Upper Witbank coal, South Africa. Org Geochem 2018;126:23–32.
[32] Peri PL, Ladd B, Pepper DA, Bonser SP, Laffan SW, Amelung W. Carbon ($\delta^{13}C$) and nitrogen ($\delta^{15}N$) stable isotope composition in plant and soil in Southern Patagonia's native forests. Glob Change Biol 2012;18(1):311–21.
[33] Skrzypek G, Jezierski P, Szynkiewicz A. Preservation of primary stable isotope signatures of peat-forming plants during early decomposition—observation along an altitudinal transect. Chem Geol 2010;273(3–4):238–49.
[34] Ali HMZ, Khan S. Ranking of Paleocene age coal salt range, Punjab and its application in coal fired power plants. Science International 2015;27 (2):1243–6.
[35] Ullah MF, Mahmood K, Akram MS. Coal mining trends and future prospects: A case study of Eastern Salt Range, Punjab. Pakistan Journal of Himalayan Earth Sciences 2018;51(2A):87–93.
[36] Rehman SU, Shah AN, Mughal HU, Javed MT, Akram M, Chilton S, et al. Geology and combustion perspectives of Pakistani coals from Salt Range and Trans Indus Range. Int J Coal Geol 2016;168:202–13.
[37] Warwick P, Shakoor T. Lithofacies and depositional environments of the coal-bearing Paleocene Patala Formation, Salt Range coal field, northern Pakistan. Project Report PK-1095 Geological Survey of Pakistan 1993.
[38] Warwick PD, Javed S, Mashhadi STA, Shakoor T, Khan AM, Khan AL. Lithofacies and palynostratigraphy of some Cretaceous and Paleocene rocks, Surghar and Salt Range coal fields, northern Pakistan. US Geological Survey 1995.
[39] Warwick PD, Wardlaw BR. Regional Studies of the Potwar Plateau Area. US Geological Survey: Northern Pakistan; 2007.
[40] Wandrey CJ, Law B, Shah HA. Patala-Nammal Composite Total Petroleum System, Kohat-Potwar Geologic Province. US Geological Survey: Pakistan; 2004.
[41] Warwick PD, Shakoor T. Preliminary report on coal characteristics in the Salt Range area of north-central Pakistan. US Geological Survey 1989.
[42] Munir MAM, Liu GJ, Yousaf B, Ali MU, Abbas Q. Enrichment and distribution of trace elements in Padhrar, Thar and Kotli coals from Pakistan: Comparison to coals from China with an emphasis on the elements distribution. J Geochem Explor 2018;185:153–69.
[43] Naveed AK, Perveen F, Habib U, Shah I. An investigation of heavy and trace elements in coal deposits of Makarwal Pakistan and their possible impacts on surrounding water-case study. Journal of Engineering and Applied Sciences 2019;38(1):38.
[44] Malik IA. Pakistan Mineral Development Corporation of Pakistan 13-H/ 9. Islamabad: The Geological Bulletin of the Panjab University; 1989.
[45] Hussain SA, Han FQ, Ma YQ, Khan H, Jian Y, Hussain G, Widory D. An overview of Pakistan rock salt resources and their chemical characterisation. Pakistan J Scientific Industrial Research Series A: Physical Sciences 2021;64(2):137–48.
[46] Ghazi S, Mountney NP, Butt AA, Sharif S. Stratigraphic and palaeoenvironmental framework of the Early Permian sequence in the Salt Range. Pakistan J Earth Syst Sci 2012;121(5):1239–55.
[47] Singh PK, Singh MP, Singh AK, Naik AS, Singh VK, Singh VK, Rajak PK. Petrological and geochemical investigations of Rajpardi lignite deposit, Gujarat. India Energy Explor Exploitation 2012;30(1):131–51.
[48] American Association for Testing of Material (ASTM). Standard Practice for Proximate Analysis of Coal and Coke. ASTM D3172-13. PA: ASTM International; 2013.
[49] Olea RA, Luppens JA. Mapping of coal quality using stochastic simulation and isometric logratio transformation with an application to a Texas lignite. Int J Coal Geol 2015;152:80–93.
[50] Shahzad M, Iqbal MM, Hassan SA, Saqib S, Waqas M. An assessment of chemical properties and hardgrove grindability index of Punjab coal. Pak J Sci Ind Res Ser A: Phys Sci 2014;57(3):139–44.
[51] Dai SF, Seredin VV, Ward CR, Hower JC, Xing YW, Zhang WG, Song WJ, Wang PP. Enrichment of U-Se–Mo–Re–V in coals preserved within marine carbonate successions: geochemical and mineralogical data from the Late Permian Guiding Coalfield, Guizhou. China Miner Deposita 2015;50(2):159–86.
[52] Ketris MP, Yudovich YE. Estimations of Clarkes for Carbonaceous biolithes: World averages for trace element contents in black shales and coals. Int J Coal Geol 2009;78(2):135–48.
[53] Dai SF, Graham IT, Ward CR. A review of anomalous rare earth elements and yttrium in coal. Int J Coal Geol 2016;159:82–95.
[54] Karayigit AI, Bircan C, Oskay RG, Türkmen İ, Querol X. The geology, mineralogy, petrography, and geochemistry of the Miocene dursunbey coal within fluvio-lacustrine deposits, Balıkesir (Western Turkey). Int J Coal Geol 2020;228:103548.
[55] Spötl C, Vennemann TW. Continuous-flow isotope ratio mass spectrometric analysis of carbonate minerals. Rapid Commun Mass Spectrom 2003;17 (9):1004–6.
[56] Widera M. Depositional environments of overbank sedimentation in the lignite-bearing Grey Clays Member: New evidence from Middle Miocene deposits of central Poland. Sediment Geol 2016;335:150–65.
[57] Hansen AE, Hower JC. Notes on the relationship between microlithotype composition and Hardgrove grindability index for rank suites of Eastern Kentucky (Central Appalachian) coals. Int J Coal Geol 2014;131:109–12.
[58] Brennan R. Coal properties dictate coal flotation strategies. Adv Mater 2011;23 (4):442–60.
[59] Malkani MS, Shah MR. Chamalang coal resources and their depositional environments, Balochistan. Pakistan J Himalayan Earth Science 2014;47 (1):61–72.
[60] Altunsoy M, Sari A, Özçelik O, Engin H, Hökerek S. Major and trace-element enrichments in the Karapınar coals (Konya, Turkey). Energy Sources A Recovery Util Environ Eff 2016;38(1):88–99.
[61] Karayiğit AI, Bircan C, Mastalerz M, Oskay RG, Querol X, Lieberman NR, et al. Coal characteristics, elemental composition and modes of occurrence of some elements in the İsaalan coal (Balıkesir, NW Turkey). Int J Coal Geol 2017;172:43–59.
[62] Ribeiro J, Flores D. Occurrence, leaching, and mobility of major and trace elements in a coal mining waste dump: The case of Douro Coalfield. Portugal Energy Geosci 2021;2(2):121–8.
[63] Hussain R, Luo KL, Zhao C, Zhao XF. Trace elements concentration and distributions in coal and coal mining wastes and their environmental and health impacts in Shaanxi. China Environ Sci Pollut Res Int 2018;25 (20):19566–84.
[64] Song D, Qin Y, Zhang J, Wang W, Zheng C. Concentration and distribution of trace elements in some coals from Northern China. Int J Coal Geol 2007;69 (3):179–91.
[65] Behera SK, Meena H, Chakraborty S, Meikap BC. Application of response surface methodology (RSM) for optimization of leaching parameters for ash reduction from low-grade coal. Int J Min Sci Technol 2018;28(4):621–9.
[66] Drew LJ, Grunsky EC, Schuenemeyer JH. Investigation of the Structure of Geological Process Through Multivariate Statistical Analysis—The Creation of a Coal. In: Proceedings of Progress in Geomathematics. Berlin, Heidelberg: Springer; 2008. p. 53–77.
[67] Oskay RG, Christanis K, Inaner H, Salman M, Taka M. Palaeoenvironmental reconstruction of the eastern part of the Karapınar-Ayrancı coal deposit (Central Turkey). Int J Coal Geol 2016;163:100–11.
[68] Liu JJ, Spiro BF, Dai SF, French D, Graham IT, Wang XB, Zhao L, Zhao JT, Zeng RS. Strontium isotopes in high- and low-Ge coals from the Shengli Coalfield, Inner

Mongolia, Northern China: New indicators for Ge source. Int J Coal Geol 2021;233:103642.
[69] Wu YY, Qin Y, Wang AK, Shen J. Geochemical anomaly and the causes of transition metal accumulations in late Permian coal from the eastern Yunnan-western Guizhou region. Int J Min Sci Technol 2013;23(1):105–11.
[70] Xu N, Peng MM, Li Q, Xu CP. Towards consistent interpretations of coal geochemistry data on whole-coal versus ash bases through machine learning. Minerals 2020;10(4):328.
[71] Xu N, Finkelman RB, Xu CP, Dai SF. What do coal geochemistry statistics really mean? Fuel 2020;267:117084.
[72] Diehl SF, Goldhaber MB, Koenig AE, Lowers HA, Ruppert LF. Distribution of arsenic, selenium, and other trace elements in high pyrite Appalachian coals: evidence for multiple episodes of pyrite formation. Int J Coal Geol 2012;94:238–49.
[73] Çelik Y, Karayigit AI, Oskay RG, Kayseri-Özer MS, Christanis K, Hower JC, Querol X. A multidisciplinary study and palaeoenvironmental interpretation of middle Miocene Keles lignite (Harmancık Basin, NW Turkey), with emphasis on syngenetic zeolite formation. Int J Coal Geol 2021;237:103691.
[74] Ding DS, Liu GJ, Sun XH, Sun RY. Response of carbon isotopic compositions of Early-Middle Permian coals in North China to palaeo-climate change. J Asian Earth Sci 2018;151:190–6.
[75] Liu BJ, Vrabec M, Markič M, Püttmann W. Reconstruction of paleobotanical and paleoenvironmental changes in the Pliocene Velenje Basin, Slovenia, by molecular and stable isotope analysis of lignites. Int J Coal Geol 2019;206:31–45.
[76] Anwita, Ghosh S, Varma AK, Das SK, Pal D, Solanki G. Metamorphic transformations of nitrogen functionalities: Stabilization of organic nitrogen in anthracite and its effect on δ15N parameter. Mar Petroleum Geol 2020;112:104090.
[77] Zheng QM, Liu QF, Huang B, Zhao WL. Isotopic composition and content of organic nitrogen in the coals of Qinshui Coalfield. North China J Geochem Explor 2015;149:120–6.
[78] Singh PK, Singh MP, Prachiti PK, Kalpana MS, Manikyamba C, Lakshminarayana G, Singh AK, Naik AS. Petrographic characteristics and carbon isotopic composition of Permian coal: Implications on depositional environment of Sattupalli coalfield, Godavari Valley. India Int J Coal Geol 2012;90–91:34–42.
[79] Holdgate GR, McGowran B, Fromhold T, Wagstaff BE, Gallagher SJ, Wallace MW, Sluiter IRK, Whitelaw M. Eocene-Miocene carbon-isotope and floral record from brown coal seams in the Gippsland Basin of southeast Australia. Glob Planet Change 2009;65(1–2):89–103.
[80] Bechtel A, Gratzer R, Sachsenhofer RF, Gusterhuber J, Lücke A, Püttmann W. Biomarker and carbon isotope variation in coal and fossil wood of Central Europe through the Cenozoic. Palaeogeogr Palaeoclimatol Palaeoecol 2008;262(3–4):166–75.
[81] Kokowska-Pawłowska M, Krzeszowska E. Assessment of possible application of geochemistry to distinguish limnic and paralic coal-bearing parts of the carboniferous in the Upper Silesian Coal Basin. Arch Min Sci 2017;62 (4):717–30.
[82] Houlton BZ, Sigman DM, Schuur EA, Hedin LO. A climate-driven switch in plant nitrogen acquisition within tropical forest communities. In: Proceedings of the National Academy of Sciences of the United States of America. National Academy of Sciences; 2007;104(21):8902–6.
[83] Kumar P. Palynological investigation of coal-bearing deposits of the Thar Coal Field Sindh, Pakistan. Lund: Lund University; 2012. Master's dissertation.
[84] Moore TA, Moroeng OM, Shen J, Esterle JS, Pausch RC. Using carbon isotopes and organic composition to decipher climate and tectonics in the Early Cretaceous: An example from the Hailar Basin, Inner Mongolia. China Cretac Res 2021;118:104674.